Carbon-Nanotubes Grown from Spin-Coated Nanoparticles for Field-Emission Displays

Do-Yoon Kim[**a], Ji-Beom Yoo[*a], In-Taek Han[b], Ha-Jin Kim[b], Ha-Jong Kim[b], Yong-Wan Jin[b], and Jong-Min Kim[b]

Abstract

The density controlled carbon nanotubes (CNTs) are grown on the iron acetate nanoparticles by using the freeze-dry method. The iron-acetate [Fe(II)(CH$_3$COO)$_2$] solution is used to prepare the catalytic iron nanoparticles. The density of CNTs is controlled in order to enhance the field emission process. Furthermore, the patterning of the iron nanoparticle catalyst-layer for the fabrication of electronic devices is simply achieved by using alkaline solution, TMAH (tetramethyl-ammonium hydroxide). We applied this patterning process of catalyst layer to form the electron emitter with under-gate type triode structure.

Keywords : CNTs, Undergate-type triode structure, Iron-acetate, freeze dry method

1. Introduction

There has significant development in both the production and application of carbon nanotubes (CNTs) since their discovery in 1991 [1], and CNTs have received considerable amount of attention during the last decade due to their unique physical and chemical properties[2~3]. In so far, a number of methods such as, laser ablation, arc discharge and catalytic pyrolysis, have been established for the synthesis of CNTs [4-6]. Among them, the method of chemical vapor deposition (CVD) has been extensively employed for the synthesis CNTs using the catalytic nanoparticle substrate. Furthermore, the CVD process has allowed the selective growth of individual CNTs and simplified the process for making of the CNT-based devices [7]. When CVD process is applied to the synthesis of CNTs, the most important factor that determine the properties of CNTs such as, the length, diameter is catalyst control [8]. In addition, the field emission characteristics are affected by the length, diameter and density of CNTs.

Properties of CNTs grown on controlled catalyst and their diversity are dominant factors of FE characteristics.

The synthesis of catalyst nanoparticles has been extensively developed due to their important role as a seed to promote CNTs growth. The synthesis of well-dispersed nanoparticles with size ranging from 2 to 10 nm enables the growth of thinner CNTs at a lower temperature. Generally, iron, nickel, cobalt metals and their alloys are used as the catalyst material to synthesize CNTs. These materials have been used in the form of thin-film as thin film catalyst is the most common and better form of catalyst to achieve selective deposition of CNTs on a desired position.

There are several ways to deposit thin film catalyst on a substrate. Physical vapor deposition (PVD) method is a commonly used method and the properties of CNTs are controlled by changing the deposition rate, temperature, thickness, and the way of combing multi layers [9]. However, it requires vacuum system and relatively complex equipment. Moreover, the step coverage is not appropriate if a very thin catalyst layer is used to decrease the CNT diameter which is intended to precisely control thin film deposition process for controlling the diameter of CNTs. Newly, organo-metallic materials coated on a substrate for making catalyst layer have been used for CNT synthesis [10-15] to overcome the disadvantage of PVD process and to easily control the catalyst characteristics. Furthermore, organo-metallic materials containing transition metals used for CNT synthesis are dissolved in

organic solvents such as ethanol, and coated on substrate by dip-coat or spin-coating method. A solution containing catalyst particles is easy to handle and does not require complex systems to coat it. However, in case of nanoparticles application instead of thin film, there are several problems with respect to the uniformity of particle distribution that need to be considered. When the particles are spread on the substrate, these particles have a tendency to agglomerate. In the present study, we have used liquid nitrogen to prevent agglomeration of catalyst particles on a substrate that take place during the drying process. The iron acetate [Fe(II)(CH$_3$COO)$_2$] catalyst solution was coated onto a glass substrate by spin-coating method and was frozen with liquid nitrogen.

After the catalyst layer was formed, we succeeded in making pattern using by TMAH (tetramethylammonium hydroxide, N(CH$_3$)$_4$OH) solution. Other techniques that can be used to produce patterned arrays relied on conventional photo or e-beam/ion beam lithography [16-19]. However, while this direct patterning method reduces the number of process step, it still makes it costly to achieve the required vacuum for the e-beam exposure and can potentially limit the throughput of such a technology. In our experiments, however, we did not need to use any vacuum equipment to make patterned arrays. This is because as the acid-base reactions are applied to the patterning process, even simple patterning methodology could be achieved.

In this study, this phenomenon of catalyst layer, which was achieved in our experiment, is adopted to propose a triode structure for FEDs with CNT emitters, designed as an under-gate triode [20] where gate electrodes are located under the cathode electrodes.

2. Experimental

First, the forming iron acetate solution was produced. We mixed iron acetate powder with ethanol. Ethanol is very soluble in iron acetate. However, at the same time, ethanol has too high a vapor pressure and low viscosity, which may cause the catalyst powder to crystallize and non-uniform morphology to occur after the drying process. Therefore, ethylene glycol was added to obtain a proper solution with low vapor pressure and high viscosity. The ethylene glycol slightly dissolved iron acetate, in order to avoid agglomeration and recrystallization during drying or heating, the

substrate covered with liquid catalyst-solution was quickly frozen in liquid-nitrogen bath. Through this process, we successfully obtained uniformly distributed catalyst particles on a substrate through this fast-freeze method. The molar concentration of the iron acetate, and volume ratio of two solvents were the experimental parameters considered to control the concentration of catalyst.

To make a triode type device, we first patterned a metal line, molybdenum (200 nm thickness, 150 μm width), on a glass substrate as a gate electrode using photolithography process. Then, SiO$_2$ layer of thickness of 3 μm was deposited by PECVD as a insulating layer. On the insulating layer, the liquid catalyst was coated by spin coater and dipped immediately into liquid nitrogen for preventing particle agglomeration. After the drying process, the catalyst film was selectively patterned by TMAH in order to form a cathode line as well as emitter. The photoresist (PR) was coated on the iron acetate layer by spin coating method. After the UV exposure through quartz mask on the iron acetate / PR double layer, substrate was immersed in the developer (TMAH). The developer was an alkali-based solution that dissolves UV-exposed PR. The UV-exposed PR and underlying iron acetate was dissolved in the developer. Iron acetate was made to react with the development solution in acid-base reaction form and then dissolved into solution. Fe^{2+} in iron acetate causes a chemical reaction to occur by the action of the base OH$^-$ in TMAH. As a result, there is no catalyst layer under the part of the PR which is illuminated by UV light. Since PR was first removed by TMAH (developer), and catalyst layer was removed next by the same TMAH. Furthermore, the iron acetate coated under-gate type triode substrate was loaded in vacuum oven, and annealed at 350-400 ℃ in air to burn the organic compound. The decomposition conditions were investigated with the thermal gravimetric analysis (TGA) and the X-ray photoelectron spectroscope (XPS). It was found that iron acetate changed into iron oxide in air, or into iron carbide in nitrogen ambient by thermal decomposition. For reference, the cathode electrode (molybdenum) on the insulating layer was used at the early stage of process. However, during the decomposition step, cathode electrode was easily peeled from the insulating layer by electrode oxidation, and so we decided to use catalyst solution of dense concentration (60 mM, 400 rpm) and make CNTs film as an emitter and cathode.

The catalyst metal (Fe) coated triode structure was

transferred into CNTs growth chamber and was consecutively heated up to 550℃ and sustained for 40 min in CO(0.5 slm) and H_2(1.0 slm) ambient. After the growth of CNTs, the field emission characteristics of triode structure with the CNT emitter were analyzed. The emission current was controlled by changing the gate voltage at a constant anode voltage. The substrate and as-grown CNTs were analyzed by atomic force microscopy (AFM, LS, PSI) and field emission scanning electron microscopy (FE-SEM, A0344, Philips).

3. Results and Discussion

The iron acetate was uniformly dispersed on the glass substrate by freeze-drying process. Particles treated by the liquid nitrogen were very effective for controlling density for CNTs growth. In the case of the freeze-dried catalyst, the catalyst, compared with conventional drying process, was immobilized by the liquid nitrogen freezing, resulting in preventing the agglomeration. Therefore, more uniform dispersion of catalyst particles and distribution of particle size were achieved in the freeze-dried catalyst process.

In addition, it is essential to achieve the patterning for the device applications. So we found out that the iron acetate catalyst layer can be selectively dissolved by the TMAH solution. That is, due to the chemical reaction of Fe^{2+} ions in iron acetate and OH⁻ ions in TMAH, the catalyst layer was removed. Actually, the first exposed PR-layer was removed by TMAH, and then the catalyst layer was removed by the same TMAH solutions.

Fig. 1 shows the SEM images of the CNTs grown on catalyst solutions with different concentrations and the coating speeds. The iron acetate concentrations (spin speed) were 20 mM (800 rpm), 40 mM (800 rpm), 60 mM (800 rpm), 60 mM (400 rpm) for a, b, c and d samples respectively, and coating time was set to ~ 10 second. In this case, the monotonic distribution of CNT diameter was observed. The denser CNT film was obtained by decreasing the coating speed from 800 to 400 rpm as shown in Fig. 1(d). We measured the field emission characteristics for the samples prepared above. It shows the effect of CNT density resulting from the catalyst concentration and coating speed on the field emission characteristics. The turn-on voltage (the applied electric field that produces the emission current of 10 $\mu A/cm^2$) of CNT film was found to decarease as the

iron acetate concentration increased from 20 mM (800 rpm) to 60mM (800rpm). However, the turn-on voltage of CNT
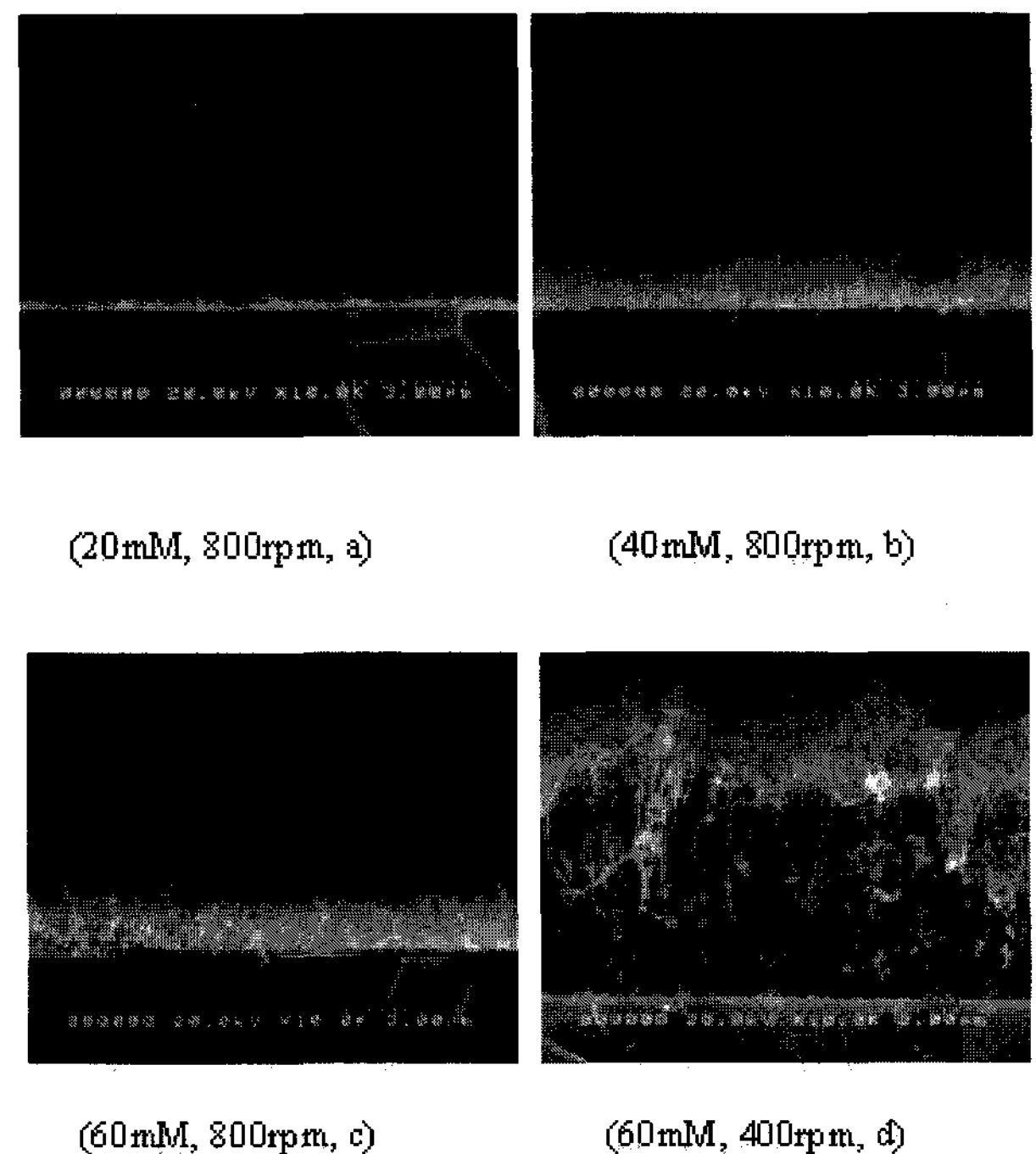

(20mM, 800rpm, a)   (40mM, 800rpm, b)

(60mM, 800rpm, c)   (60mM, 400rpm, d)

Fig. 1. CNTs grown from 20 mM(800rpm), 40 mM(800 rpm), 60 mM(800 rpm) and 60 mM(400 rpm) catalyst solution prepared by the freeze-dried method.

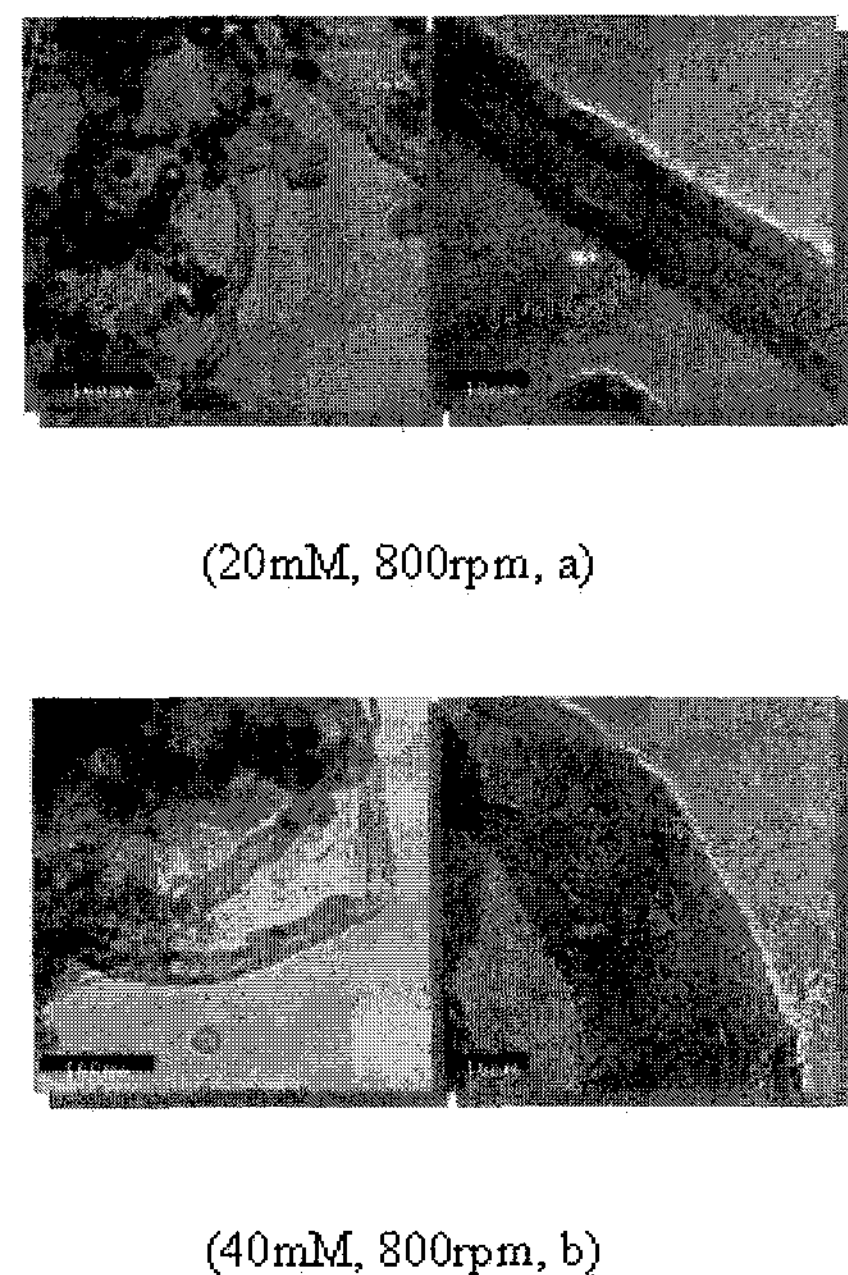(20mM, 800rpm, a)

(40mM, 800rpm, b)

Fig. 2. TEM images of the CNTs grown from 20 mM(800 rpm), 40 mM(800 rpm).

was found to increase as the thickness of catalyst increased by the decrease in the coating speed from 800 to 400 rpm. The turn-on voltage of the samples (a), (b), (c) and (d) were 5.76 V/μm, 4.48 V/μm, 3.56 V/μm and 3.68 V/μm, respectively. The AFM analysis show, the thickness of catalyst layer for samples (a), (b), (c) and (d) were 70 Å, 150 Å, 330 Å and 630 Å. The field enhancement factor, β, values were also changed to 699, 2917, 4485 and 2862. These results indicate that, there exists an optimum density of CNTs, which can be controlled by varying the iron acetate concentration and the coating conditions. Based on this, it can be concluded that, lower turn-on voltage can be obtained by precise control of the iron acetate concentration on substrate surface.

Figs. 2 (a) and (b) show the TEM images of the CNTs grown on catalyst solutions with different concentrations. The iron acetate concentrations (spin speed) were (a) 20 mM (800 rpm) and (b) 40 mM (800 rpm). The diameter of the CNTs grown on sample (a) is 12nm, and CNTs which have 25 nm-diameter were formed from the sample (b).

For a full-scale imaging and a fast response for moving pictures, a triode structure is necessary. Fig. 3 shows the schematic diagram of a triode structure with carbon nanotube emitters and electric potential distributions and trajectories near the cathode electrodes depending on gate voltages. This electric potential distributions and
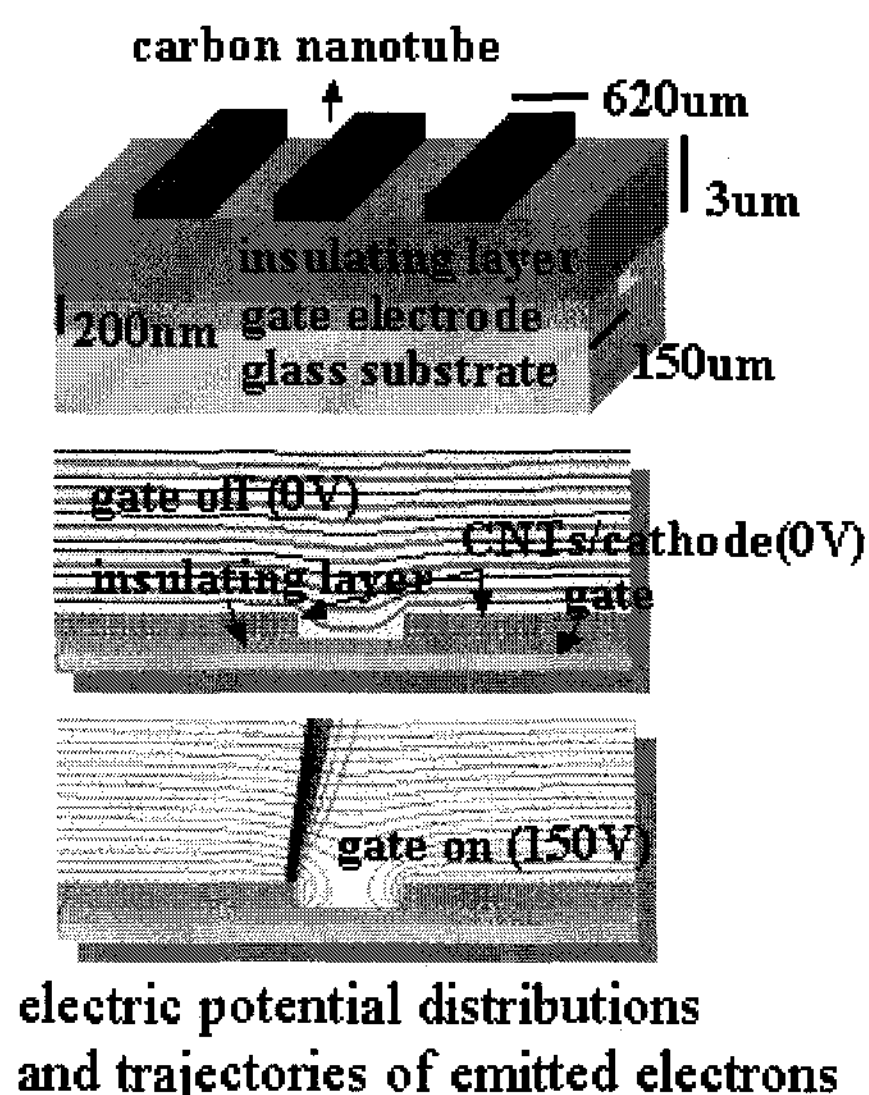
electron trajectories near the cathode electrodes were calculated using the commercial software SIMION. In the triode structure, electrons are first field-emitted from the cathode by a gate voltage and then attracted to the anode. The gate electrodes in a normal triode structure are located above the cathode electrode, which enables the emission electrons to easily reach the anode electrode. But in our cases, the gate electrode was under the cathode, on the opposite side of the anode. Using this structure, we obtained a simple form of the structure and the fabrication process which seems to enable the under-gate type triode to possess high potential for practical applications.

In this under-gate triode structure, it is well known that the electric field strength is concentrated at the edges of the cathode electrodes. This causes the electron emission to turn on and off depending on the gate voltages for a given anode voltage. Thus, this under-gate triode structure also has the advantage of preventing broad electron emission.

Fig. 4 shows the optical microscope image and the SEM images of a triode structure. Fig. 4 (a) shows two lines crossing at right angles. Horizontal lines denote gate electrodes while the perpendicular lines represent cathode electrodes and a catalyst layer. There are insulating layer between two electrodes. Figs. 4 (b) and (c) show a cross-sectional SEM images of the triode structure with CNT emitters. The catalyst layers were coated on substrate by spin-coating 60 mM iron-acetate solution of 400 rpm.

Fig. 5 shows the real images of the triode sample. Before and after CNTs growth process, we could see the CNTs and cathode line on the insulating layer.

Fig. 6 shows, the current-voltage characteristics of the triode in the triode mode. Fig. 6 (a) shows the emission characteristics of CNT emitters with a diode configuration.
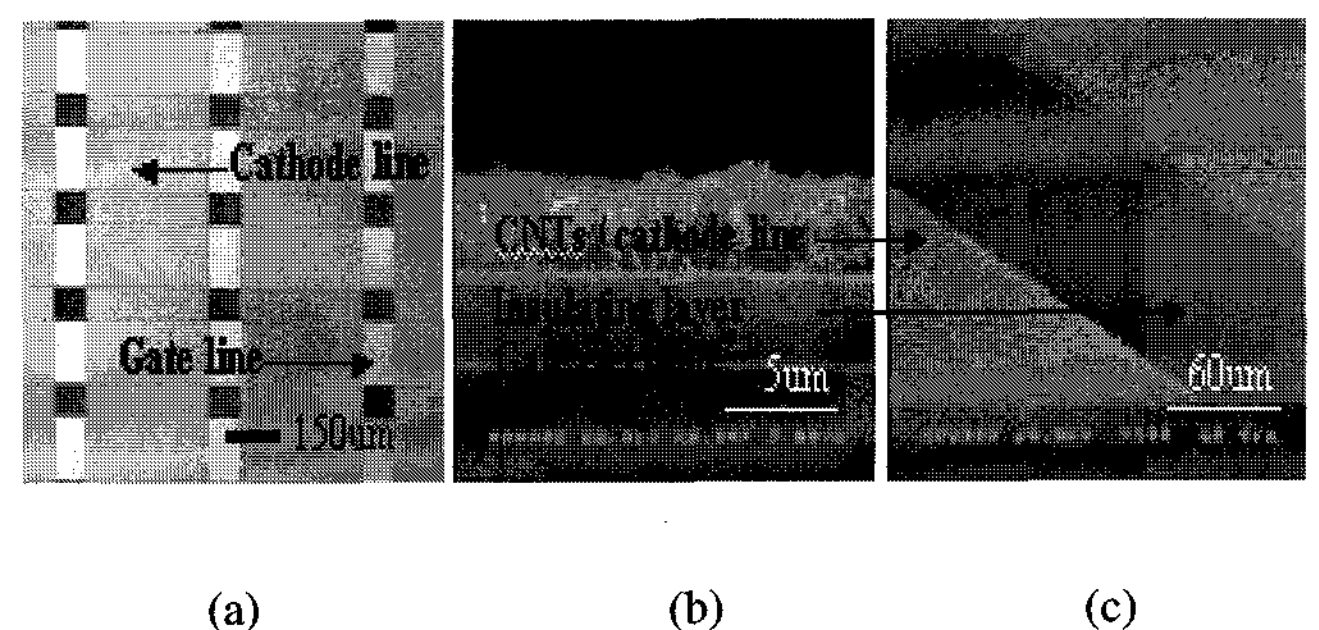

Fig. 3. Schematic diagram of a triode structure with the carbon nanotube emitters and the electric potential distributions and the trajectories of the emitted electron near the cathode electrodes with and without gate voltage.

(a) (b) (c)

Fig. 4. An optical microscope image and SEM images of triode structure.

The maximum current density is ~ 2 mA/cm^2 and the turn-on voltage is ~ 3.6 V/μm. In Fig. 6 (b), the anode voltage is set at 800 V, which is a little lower than the turn-on voltage of ~ 900 V for the anode voltage in the diode mode. At a cathode-anode gap of ~ 1000 um, we could obtain
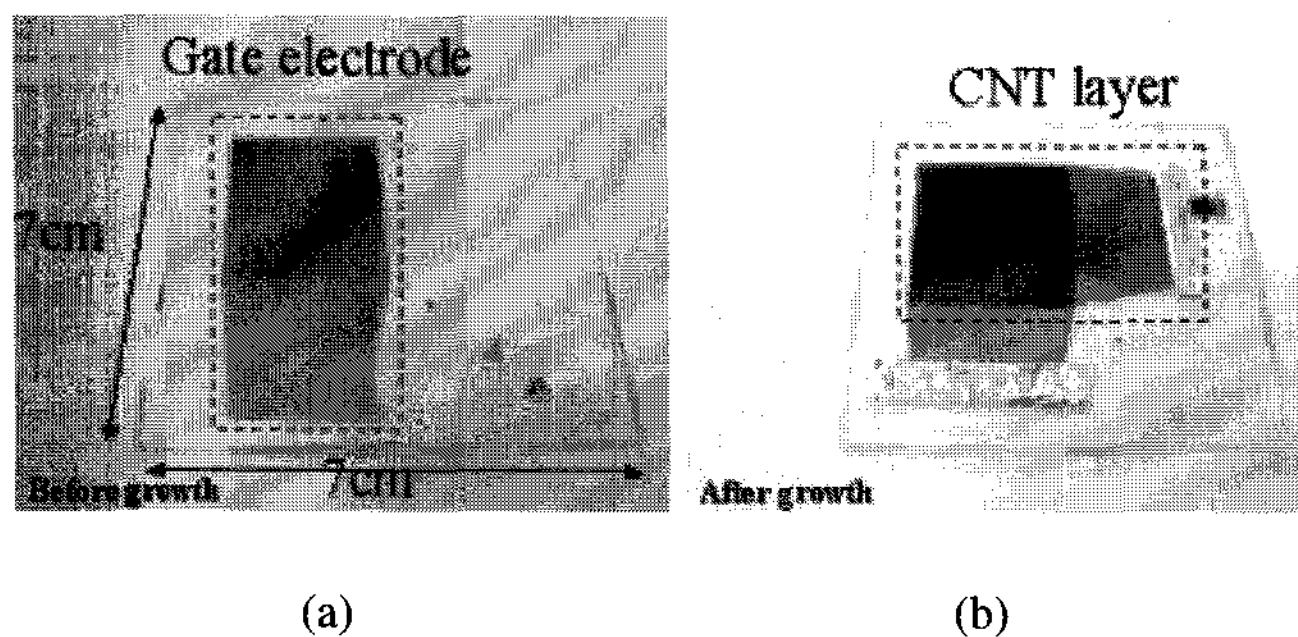

(a)   (b)

Fig. 5. Images of the device (a) before and (b) after CNTs growth process.
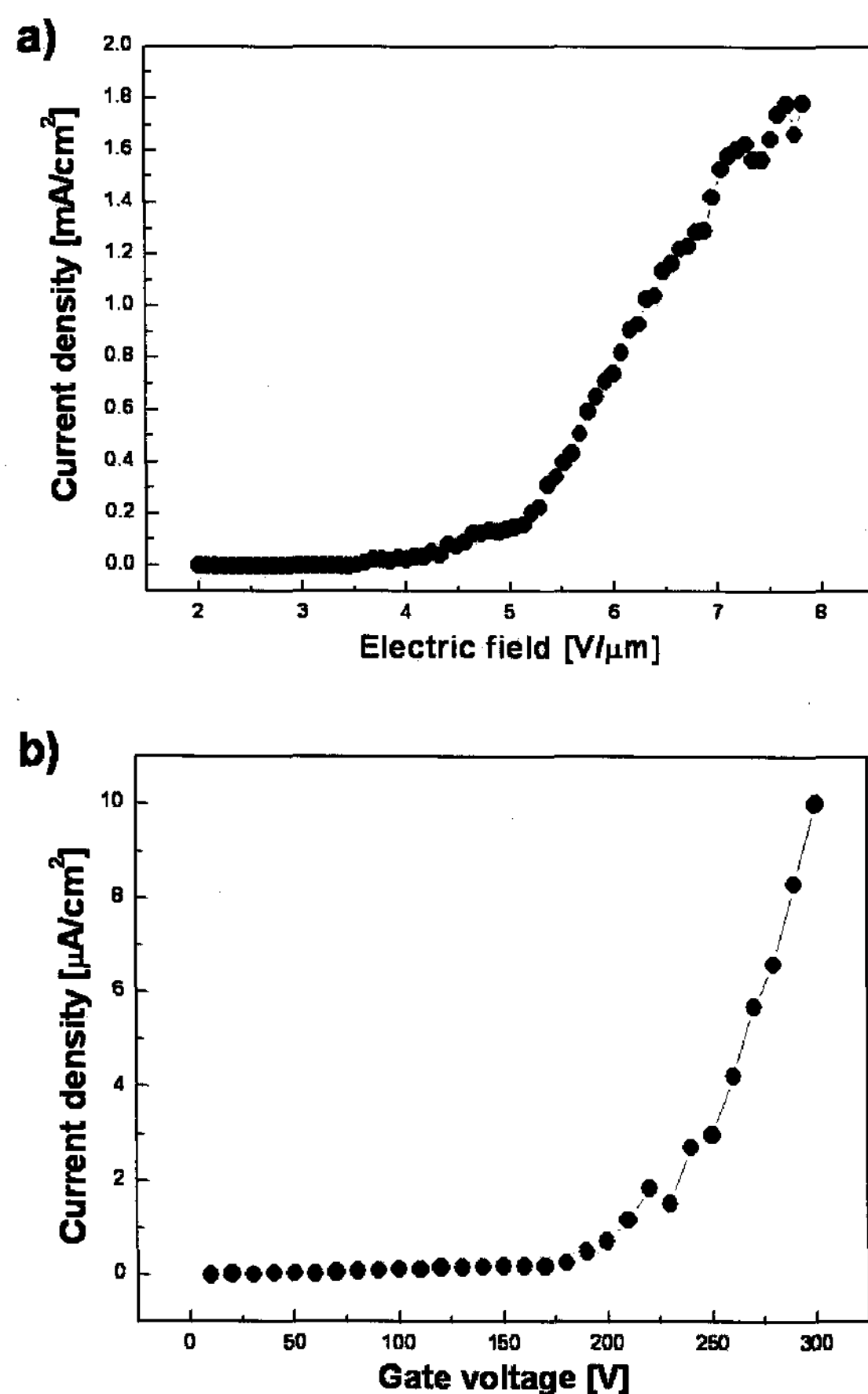

Fig. 6. I-V characteristics for a triode structure in (a) diode and (b) triode modes, where the gate electrodes are electrically floated in the diode mode and the anode electrode is set to be 800 V in the triode mode.

approximately 250 V turn-on voltage in a triode mode. However, this measurement of turn-on voltage in the triode mode is much higher than expected. This result is due to the concentration or the density of the CNT emitters. Although our structure has high turn-on voltage, this study is still worthy to take note because. Furthermore, the triode structure in our experiment with liquid catalyst has assured advantages of its simple structure and fabrication process.

4. Conclusion

We have fabricated the under-gate type triode structure using carbon nanotubes grown from the iron nanoparticles as electron emission sources and characterized their field emission properties. The freeze-drying process for uniform distribution of catalyst particles was also applied to the triode structure to form a catalyst layer. From this study, we successfully verified that electron emission is operated by the modulation of gate voltages. Although there are some technical issues that need to be solved, the fact that a catalyst layer is formed by the fast-freeze method in itself is meaningful. Thus, further research need to be conducted on the applicability of its device.

References

[1] S. Iijima, *Nature,* **354**, 56 (1991).
[2] P. G. Collins, A. Zettle, H. Bando, A. Thess, and R. E. Smally, *Science,* **278**, 100 (1997).
[3] A.C. Dillon, K. M. Jones, T. A. Bekkedahl, C. H. Kiang, D. S. Bethune, and M. J. Heben, *Nature,* **386**, 377 (1997).
[4] C. A. Bower, O. Zhou, Z. Wei, D. J. Werder, and J. Sungho, *Appl. Phys. Lett.,* **77**, 2767 (2000).
[5] M. Chhowalla, K. B. K. Teo, C. Ducati, N. L. Rupesinghe, G. A. J. Amaratunga, A. C. Ferrari, D. Roy, J. Robertson, and W. I. Milne, *J. Appl. Phys.,* **90**, 5308 (2001).
[6] M. Croci, J.-M. Bonard, O. Noury, T. Sto"ckli, and A. Chatelain, *Chem. Vap. Deposition,* **8**, 89 (2002)
[7] S. J. Oh, J. Zhang, Y. Cheng, H. Shimoda, and O. Zhou, *Appl. Phys. Lett.,* **84**, 3738 (2004).
[8] C. Ducati, I. Alexandrou, M. Chhowalla, J. Robertson, and G. A. J. Amaratunga, *J. Appl. Phys.,* **95**, 6387 (2004).
[9] Ruth Y. Zhang, I. Amlani, J. Baker, John Tresek, Raymond K. Tsui, and P. Fejes, *Nano Lett.,* **3**, 731 (2003).
[10] Y. Murakami, Y. Miyauchi, and S. Maruyama, *Chem. Phys. Lett.,* **377**, 49 (2003).
[11] S. Maruyama, R. Kojima, Y. Miyauchi, S. Chiashi, M.

Kohno, *Chem. Phys. Lett.,* **360**, 229 (2002).

[12] Ruth Y. Zhang, Islamshah Amlani, Jeff Baker, John Tresek, and Raymond K. Tsui, *Nano Lett.,* **3**, 731 (2003).

[13] Y. Murakami, Y. Miyauchi, S. Chiashi, and S. Maruyama. *Chem. Phys.Lett.,* **374**, 53 (2003).

[14] L. Nilsson, *Appl. Phys. Lett.,* **76**, 2071 (2000).

[15] N. Nagaraju, A. Fonseca, Z. Konya, and J. B. Nagy, *J. of Molecular Catalysis A,* **181**, 57 (2002).

[16] R.M.H. New, R.F.W. Pease, and R.L. White, *J. Vac. Sci.* *Technol. B,* **13**, 1089 (1995).

[17] A.Y. Toporov, R.M. Langford and A.K. Petford-Long, *App. Phys. Lett.,* **77**, 3063 (2000).

[18] U.C. Fisher, and H.P. Zingsheim, *J. Vac. Sci. Technol.,* **19**, 881 (1981).

[19] C.A. Ross, *Annu. Rev. Mater. Res.,* **31**, 203 (2001).

[20] Y.S. Choi, J.H. Kang, Y.J. Park, W.B. Choi, C.J. Lee, S.H. Jo, C.G. Lee, J.H. You, J.E. Jung, N.S. Lee, and J.M. Kim., *Diamond & Related Materials,* **10**, 1705 (2001).